SciMedCentral

JSM

Biotechnology & Biomedical Engineering

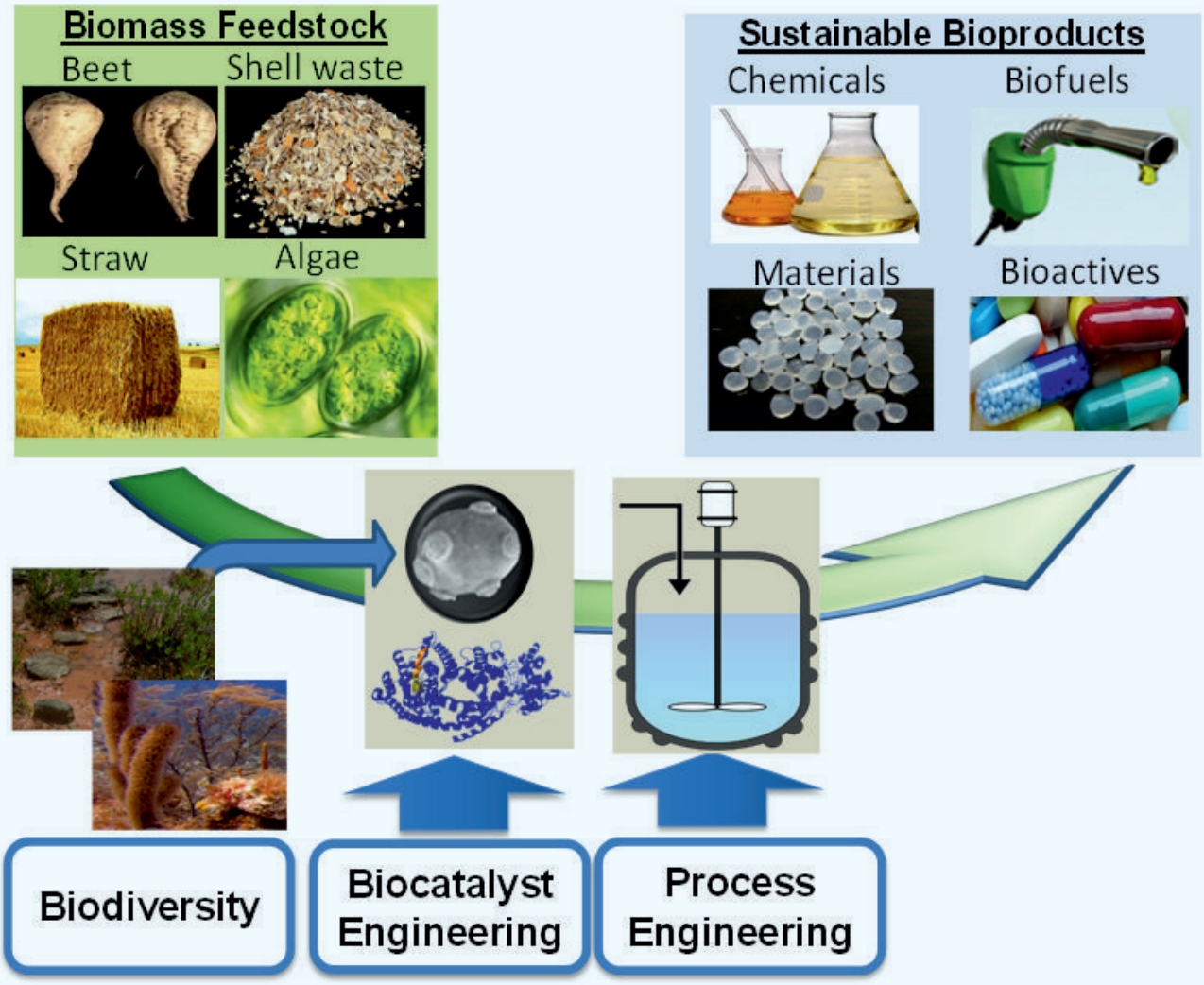

Special Issue on

Industrial Biotechnology-Made in Germany: The path from policies to sustainable energy, commodity and specialty products

Edited by:

Dr. Thomas Brück

Professor of Industrial Biocatalysis, Dept. of Chemistry, Technische Universität München (TUM), Germany

Research Article

Biosynthesis of Ginsenosides in Field-Grown *Panax Ginseng*

Schramek, N.[1], Huber, C.[1], Schmidt, S.[1], Dvorski, S.E.[1], Kmispel, N.[1], Ostrozhenkova, E.[1], Pena-Rodriguez, L.M.[1,2], Cusido, R.M.[3], Wischmann, G.[4] and Eisenreich, W.[1]*

[1]*Lehrstuhl für Biochemie, Technische Universität München, Germany*
[2]*Laboratorio de Química Orgánica, Centro de Investigación Científica de Yucatán, México*
[3]*Laboratorio de Fisiología Vegetal, Facultad de Farmacia, Universidad de Barcelona, Spain*
[4]*FloraFarm GmbH, Walsrode-Bockhorn, Germany*

Abstract

The biosynthesis of the triterpenoid ginsenosides Rg_1 and Rb_1 was studied by $^{13}CO_2$ pulse-chase experiments in six-year-old *Panax ginseng* growing in the field. A pulse period of 7 hours followed by a chase period of 8 days was shown to generate significant ^{13}C-enrichments in both ginsenosides (Rg_1> Rb_1), as well as in free sugars and amino acids. More specifically, $^{13}CO_2$-labeled Rg_1 and Rb_1 were characterized by specific NMR couplings due to$^{13}C_2$-units indicating the mevalonate origin of the triterpenes. $^{13}C_3$-Labeled motifs in Rg_1 or Rg_1 that should be generated by the alternative methylerythritol phosphate pathway from a $^{13}C_3$-triose phosphate precursor were apparently absent, whereas $^{13}C_3$-isotopologues were detected in free sugars, amino acids and the sugar moieties of the ginsensosides from the same experiment. It can be concluded that ginsenosides are predominantly or entirely biosynthesized in *P. ginseng* via the mevalonate route, under the physiological conditions of the field experiment. The observed labeling patterns were also in perfect agreement with a chair-chair-chair-boat conformation of the (S)-2,3-oxidosqualene precursor entering the cyclization process with the dammarenyl intermediate. The higher enrichments of $^{13}C_2$-isotopologues in the protopanaxatriol-type Rg_1 in comparison to the protopanaxadiol-type Rb_1 indicated higher rates of Rg_1 biosynthesis during the pulse/chase experiment with the six-year-old plant of *P. ginseng*. In summary, the study reveals the nature and dynamics of the ginsenoside biosynthetic pathway as a welcome basis for future biotechnological means.

***Corresponding author**
Prof.Dr. Wolfgang Eisenreich, Lehrstuhl für Biochemie, Technische Universität München, Lichtenbergstr. 4, 85747 Garching, Germany, Tel: +49-89-289-13336; Fax: +49-89-289-13363; E-Mail: wolfgang.eisenreich@ch.tum.de

Submitted: 14 April 2013
Accepted: 12 May 2014
Published: 14 May 2014
ISSN: 2333-7117

Keywords
- Araliaceae
- Triterpene
- Mevalonate
- Isotopologue Profiling
- $^{13}CO_2$

INTRODUCTION

Medicinal plants are important sources of therapeutics aimed at alleviating human disease. With increasing awareness of the health hazards and toxicity associated with the indiscriminate use of synthetic drugs and antibiotics, interest in plant-based drugs has revived throughout the world [1]. The World Health Organization has estimated that more than 75 % of the population in developing countries depends primarily on traditional herbal medicine for basic healthcare needs and the worldwide annual market for these products approached about US $ 60 billion [2-3]. Based on the current research, world-wide strategies and financial investments, it can be assumed that medicinal plants will continue to play an important role in health care [4].

Ginseng (*Panax ginseng* C.A. Meyer), belonging to the Araliaceae family, is one of the most important plants in traditional and modern East Asian Medicine. Since centuries, Ginseng extracts are used for anti-aging, anti-oxidative, adaptogenic and other health-benefitting effects [5,6]. Not surprisingly, Ginseng has now also been established in the phytotherapy of Western Medicine [7].

Although some advances in the production of ginsenosides by tissue culture and biotransformation have been made recently [8-10], Ginseng drugs are mostly based on extracts from the roots of four to seven year-old *Panax* plants grown in the field, e.g. in South Korea, China, Canada, and the US. These cultivations produce about 80,000 tons of fresh Ginseng roots per year. The world Ginseng market has been estimated to be around US$ 2,000 million [7].

The multiple effects of Ginseng on human health are intensely studied but still not completely understood [5,11-25]. Its bioactivity is mainly assigned to ginsenosides, a group of triterpene saponins that are unique to *Panax* plants and especially abundant in the roots of *P. ginseng*. In the meantime, more than 150 different ginsenosides are known [13,24,26-28]. Most of them belong to the dammarane or the oleanane-type, respectively (Figure 1). According to their glycone moieties, dammarane-type ginsenosides are further classified into protopanaxadiol-type ginsenosides (for example, Rb_1) and protopanaxatriol-type ginsenosides (for example, Rg_1) (Figure 1). Recently, suppressive effects of Rg_1 on liver glucose production could be determined in HepG2 human hepatoma cells *via* the LKB1-AMPK-FoxO1 pathway [29]. Moreover, Rg_1 and especially Rb_1 showed beneficial cell-protective effects in models for ischemic disease [30-31], oxidative cellular stress [32], and hyper permeability-related diseases induced by bacterial pathogens [33].

Despite the enormous pharmacological importance of these compounds, the biosynthesis of ginsenosides is not completely understood [9,24,34-38]. Generally, triterpenoid saponins are

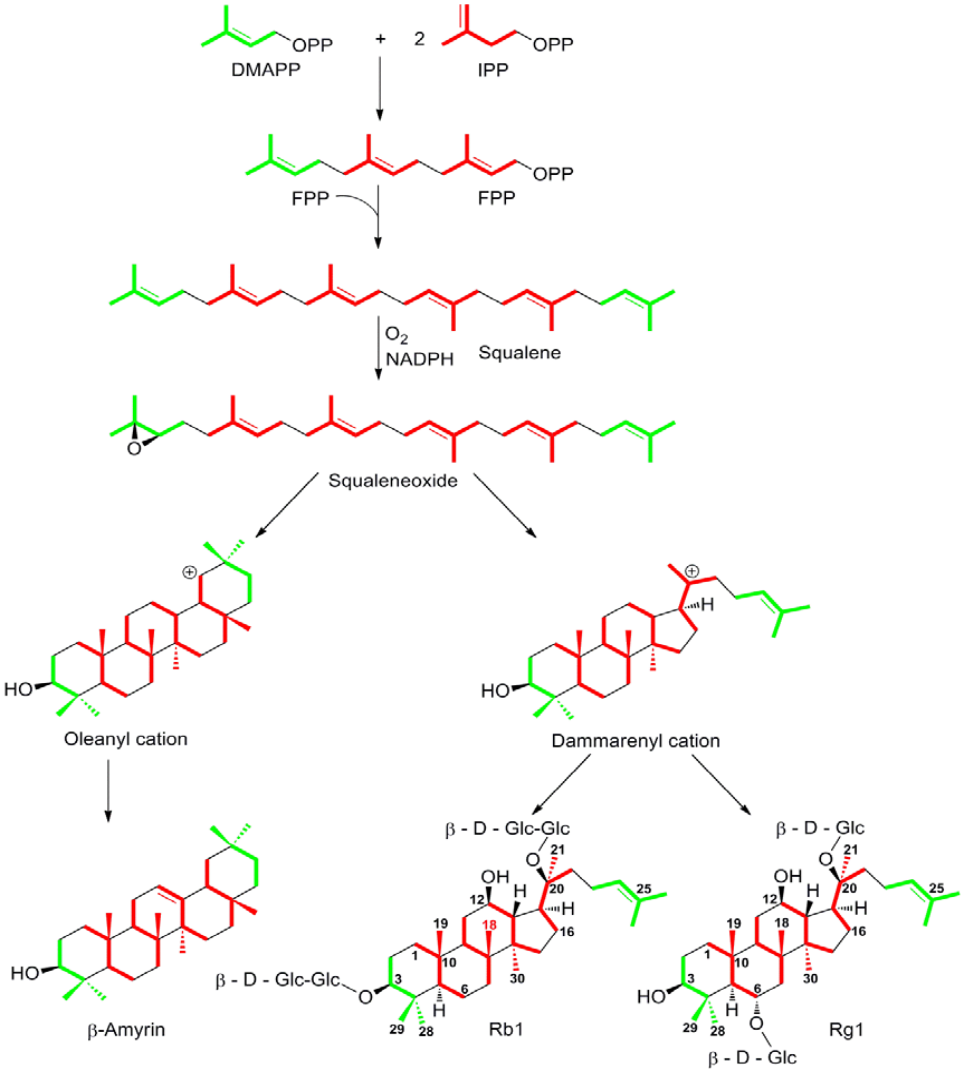

Figure 1 Formation and isoprenoid dissection of β-amyrin and ginsenosides Rb_1 and Rg_1. Carbon atoms derived from DMAPP and IPP are indicated in green and red, respectively. The used carbon numbering of Rb_1 and Rg_1 is also indicated.

believed to be derived from the linear C_{30} compound, squalene, made by the head-to-head condensation of two molecules of farnesyl diphosphate (FPP), each of them assembled from dimethylallyl diphosphate (DMAPP) and two molecules of isopentenyl diphosphate (IPP) [8]. In an O_2-dependent process, squalene is converted into (S)-2,3-oxidosqualene [39] which reacts to dammarane [40-43] or oleanane (β-amyrin) [44-45] triterpenes. These intermediates are then converted into ginsenosides by multiple oxidations (e.g. catalyzed by cytochrome P_{450}-dependent monooxygenases) [46-48] and glycosylations [34,36] which are largely unknown (Figure 1).

Also less understood is the generation of the early precursors IPP and DMAPP used in the biosynthesis of triterpenes including ginsenosides. Generally, these early precursors are formed in the cytosolic compartment of plant cells by the classical mevalonate pathway (Figure 2A). Three molecules of acetyl-CoA produce 3-hydroxy-3-methylglutaryl-CoA (HMG-CoA) which is reduced to mevalonate. By phosphorylation and decarboxylation/elimination, mevalonate is finally converted into IPP which can be isomerized to DMAPP [49-52].

However, in the plastidic compartment of plant cells, also a mevalonate-independent pathway (methylerythritol phosphate pathway, MEP pathway) exists for the biosynthesis of IPP and DMAPP (Figure 2B). This pathway starts with the condensation of glyceraldehyde 3-phosphate (GAP) and a C_2-unit from pyruvate affording 1-deoxy-D-xylulose 5-phosphate (DXP). DXP is then rearranged and reduced to 2-*C*-methyl-D-erythritol 4-phosphate (MEP), which leads via four steps to (*E*)-4-hydroxy-3-methyl-but-2-enyl diphosphate (HMBPP). In the final reaction, HMBPP is reduced to a mixture of IPP and DMAPP [53-56].

Due to the assignment of the mevalonate and MEP pathway to the cytosolic or plastidic compartments, respectively, plant terpenes made in the cytosol (e.g. phytosterols) are thought to be derived from the mevalonate pathway, whereas terpenes formed in the plastids (e.g. monoterpenes, diterpenes and carotenoids) are believed to be made from the MEP route.

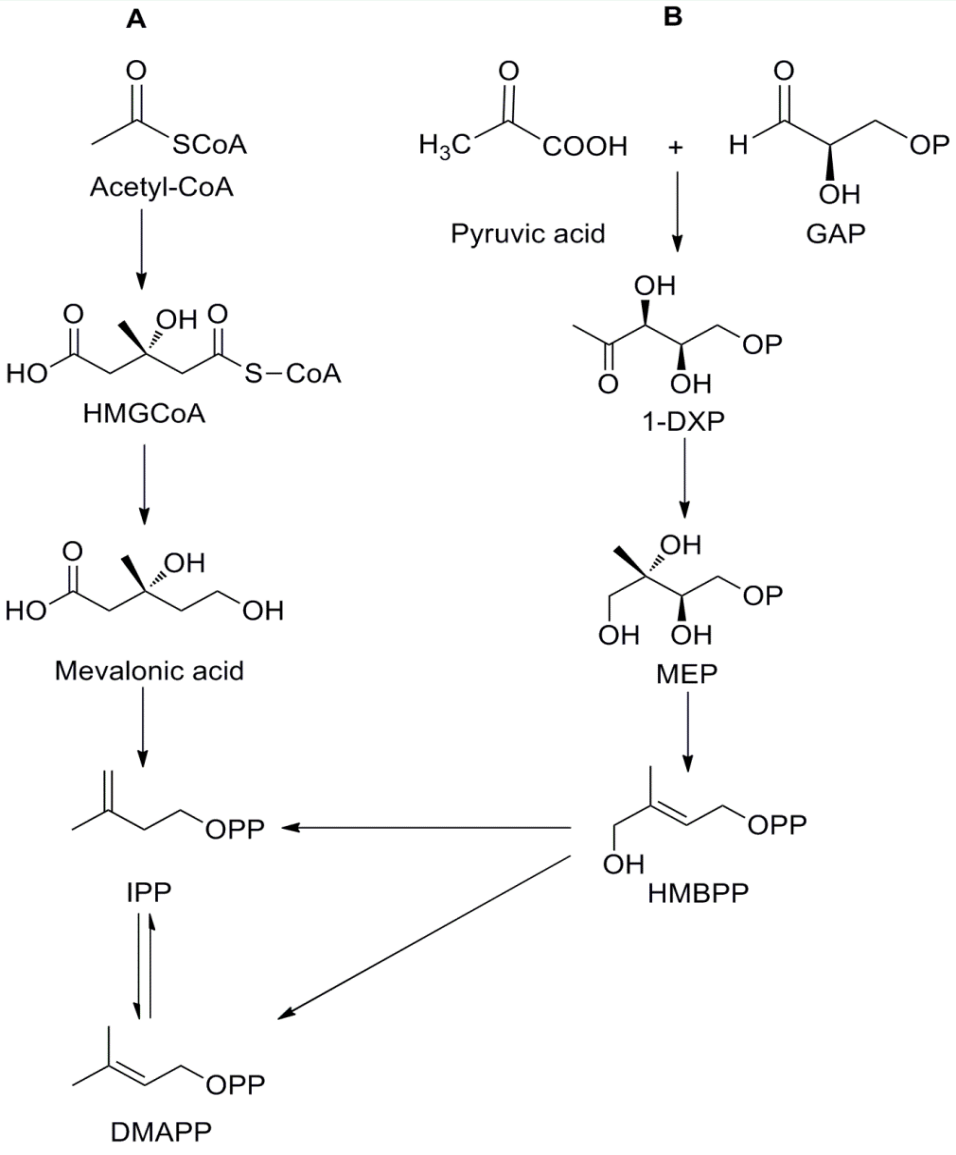

Figure 2 Biosynthetic origin of IPP and DMAPP via the mevalonate pathway (A) and the alternative MEP pathway (B).

Indeed, this classification has now been approved experimentally for many terpenes, mainly on the basis of labeling experiments with plant cell cultures (reviewed in [56]). On the other hand, exchange of mevalonate or MEP-derived precursors between the compartments has been observed affording plant terpenes with mixed biosynthetic origin [57-62].

The biosynthesis of ginsenosides occurs in the cytosolic compartment, and, on this basis, a cytoplasm-located mevalonate origin of the precursors can be assumed. However, direct experimental evidence for the biosynthetic assignment of triterpenes is scarce. Recently, the lupeol moiety in lupeol-3-(3'-*R*-hydroxy)-stearate has been shown to exclusively originate from the mevalonate pathway in the Yucatan plant, *Pentalinon and rieuxii* [63]. On the other hand, the biosynthesis of the dinortriterpenoid withanolides from *Withania somnifera* has been reported to involve both the mevalonate and the MEP route [64]. The same conclusion was made from recent experiments with hairy root cultures of *P. ginseng* exposed to mevinolin or fosmidomycin, specific inhibitors of the mevalonate or the MEP pathway, respectively [65]. However, it became not clear from the later study whether this mixed contribution is also valid for ginsenoside formation in whole plants of *Panax*.

In the present work, we have labeled full-grown plants of *P. ginseng* under field conditions using $^{13}CO_2$ as a tracer. Indeed, this method allows the maintenance of physiological conditions during the labeling experiment with a minimum of stress factors for the plant [66]. During the incubation period with $^{13}CO_2$ for several hours (pulse phase), the photosynthetic generation of completely ^{13}C-labeled metabolic intermediates (e.g. triose and pentose phosphates) takes place. During a subsequent chase phase where the plants are further cultivated under standard conditions for several days (i.e. in a natural atmosphere

containing $^{12}CO_2$), unlabeled photosynthetic intermediates are generated. The combination of these ^{13}C- and ^{12}C-intermediates as precursor units for downstream biosynthetic processes then yields a specific mixture of ^{13}C-labeled and unlabeled fragments in the product [57,67-69]. Recent improvements in GC/MS and NMR technology have allowed the deconvolution of these complex isotopologue patterns aimed at the elucidation of biosynthetic pathways and fluxes.

We here show that the experimental approach can also be used to study the biosynthesis of ginsenosides in full-grown plants of *P. ginseng*. A relatively short $^{13}CO_2$ pulse (i.e. 7 hours) followed by a chase period of 8 days resulted in specific ^{13}C-labeling patterns in the major ginsenosides Rg_1 and Rb_1 from the roots. High-resolution NMR spectroscopy revealed ^{13}C-coupling profiles that documented the mevalonate origin of these compounds.

MATERIALS AND METHODS

Chemicals

$^{13}CO_2$ (99 % ^{13}C-abundance) and other chemicals were obtained from Sigma-Aldrich (Steinheim, Germany). Reference samples for Rb_1 and Rg_1 were obtained from Roth (Karlsruhe, Germany).

Plants and $^{13}CO_2$ experiment

Labeling experiments with $^{13}CO_2$ were carried out in August 2011 using six-year-old plants of *Panax ginseng* C.A. Meyer growing in the commercial field of FloraFarm GmbH (Walsrode-Bockhorn, Germany). The labeling unit [66] was based on a chamber consisting of a clear-transparent plastic sheet around a wire-mesh cylinder that can be flushed with synthetic air and/or $^{13}CO_2$ from reservoir gas containers (Figure 3A). The chamber was tightened around the bottom stem of the plant. The concentrations of $^{12}CO_2$ and $^{13}CO_2$ were monitored online using a gas analyzer (Advance Optima, ABB, Mannheim, Germany). The $^{13}CO_2$ dosage unit was controlled by a pressure reduction valve reducing the $^{13}CO_2$ pressure coming from the cylinder to about 300 to 500 mbar. An electronic valve then controlled the influx of $^{13}CO_2$ into the incubation chamber according to the target value inside the chamber (i.e. 700 ppm $^{13}CO_2$). To reduce the $^{12}CO_2$ content during incubation, the chamber was eventually flushed with synthetic air. Inflow of synthetic air was electronically controlled depending on the target value for the $^{12}CO_2$ content (typically < 70 ppm).

Using this setting, the *P. ginseng* plant was kept under the $^{13}CO_2$ atmosphere (700 ppm $^{13}CO_2$) for 7 h from 10 a.m. until 5 p.m. ($^{13}CO_2$ throughput, about 20 L). After this pulse period, the plant was left for 8 days (chase period) under the natural field conditions. Then, the plant was harvested including the roots (Figure 3B). The leaves and roots were washed, cut in pieces, frozen (liquid nitrogen) and lyophilized. The dry root pieces were subsequently ground using a mortar and a Retsch ZM 1 mill (Haan, Germany).

Analytical HPLC of ginsenosides

Analysis of ginsenosides was carried out according to the monograph on Ginseng in the European Pharmacopoeia [70]. Approximately 100 mg of dry root powder was extracted two times by boiling with each 7 mL of 50 % methanol. The combined methanol fractions were evaporated to dryness and the residue was dissolved in 20 mL of 20 % aqueous acetonitrile. HPLC analysis was performed using a Symmetry C_{18} 150 x 3.9 mm column (Waters, Eschborn, Germany) with a flow rate of 1 mL/min. The injection volume was 20 µL. Within 40 min, a gradient from 20 % to 40 % aqueous acetonitrile was applied, followed by an increase to 100 % acetonitrile within 7 min. The eluate was monitored at 203 nm using a UV detector.

Large-scale extraction of ginsenosides

Figure 3 **(A)** – Portable unit used for $^{13}CO_2$-labeling of *P. ginseng* under field conditions (B) – Roots of $^{13}CO_2$-labeled *P. ginseng* that yielded the ginsenosides Rg_1 and Rb_1 described in this study.

The dry root powder (10 g) was extracted with 100 mL of methanol for 2 h in a Soxhlet extractor. The extract was concentrated to 5 ml under vacuum and centrifuged (14.000 rpm, 3 min). The supernatant was subjected to preparative HPLC chromatography.

Purification of ginsenosides by preparative HPLC

The major ginsenosides Rb_1 and Rg_1 were purified by preparative HPLC (Merck Hitachi) on a reversed phase column (Luna® 5 µm C_{18} (2) 100 Å AX; 150 x 21.2 mm; Phenomenex, Aschaffenburg, Germany) with a flow rate of 8 ml/min. Within 40 min, a gradient from 15 % to 40 % aqueous acetonitrile was applied, followed by an increase to 100 % acetonitrile within 5 min. The eluate was monitored at 206 nm using an UV detector. The retention volumes of Rg_1 and Rb_1 were 200 and 305 ml, respectively. Fractions containing Rg_1 and Rb_1 were concentrated to dryness under reduced pressure and subjected to NMR analysis.

NMR spectroscopy of ginsenosides

100 mg of Rg_1 or 50 mg of Rb_1 were dissolved in 600 µL of methanol-D_4 and subjected to one- and two-dimensional NMR analysis. ^{13}C NMR spectra were measured with a Bruker Avance-III 500 MHz spectrometer equipped with a cryo probe (5 mm CPQNP, $^{1}H/^{13}C/^{31}P/^{19}F/^{29}Si$; Z-gradient). ^{1}H NMR spectra were registered with an Avance-I 500 MHz system and an inverse probe head (5 mm SEI, $^{1}H/^{13}C$; Z-gradient). The temperature was 300 K. Data processing and analysis was done with TOPSPIN 3.0 or MestreNova. The one-dimensional ^{13}C NMR spectrum as well as COSY, TOCSY, HSQC, HMBC, INADEQUATE and 1,1-ADEQUATE spectra were measured with standard Bruker parameter sets. ^{13}C abundances were determined via the ^{13}C-coupled satellites in ^{1}H NMR spectra. Multiple-labeled isotopologues displaying $^{13}C^{13}C$-couplings were quantified from the corresponding satellite signals in the ^{13}C NMR spectra. The integral of each respective satellite pair was referenced to the total signal integral of a given carbon atom.

GC/MS analysis of amino acids

5 mg of the freeze dried root sample was suspended in 0.5 ml of 6 M HCl and incubated for 24 h at 105 °C. Afterwards, HCl was removed under nitrogen supply, and 200 µl of glacial acetic acid was added to the dried sample. The hydrolysate was transferred onto a mini-column of Dowex 50WX8 (H^+ form; 200 to 400 mesh; 0.5 x 1 cm). The column was washed twice with water and developed with 1 ml of 4 M ammonium hydroxide. An aliquot of the eluate was dried under a stream of nitrogen, and the residue was dissolved in 50 µl of dry acetonitrile. A total of 50 µl of *N*-(*tert*-butyldimethylsilyl)-*N*-methyltrifluoracetamide containing 1 % *N*-(*tert*-butyldimethylsilyl chloride (TBDMS; Sigma-Aldrich, Steinheim, Germany) was added. The mixture was kept at 70 °C for 30 min. The resulting mixture of TBDMS amino acids was used for GC/MS analysis that was performed on a GC-QP 2010 plus (Shimadzu, Duisburg, Germany) equipped with a fused silica capillary column (equity TM-5; 30 m by 0.25 mm, 0.25 µm film thickness; Supelco, Bellafonte, PA). The mass detector worked in electron ionization (EI) mode at 70 eV. An aliquot of the solution was injected in split mode (1:10) at an injector and interface temperature of 260 °C. The column was held at 150 °C for 3 min and then developed with a temperature gradient of 7 °C/min to a final temperature of 280 °C. The retention time of alanine-TBDMS under these conditions was 6.2 min. Samples were analyzed in SIM mode at least three times. Data were collected with Lab Solution software (Shimadzu, Duisburg, Germany). The overall ^{13}C excess values and the isotopologue compositions were calculated by an Excel-based in-house software package.

GC/MS analysis of sugars

Sugars were analyzed as diisopropylidene-acetate derivatives. 10 mg of the freeze dried root or leaf sample were incubated for 1 h at room temperature with 1 ml of acetone containing 20 µl H_2SO_4. 2 ml of saturated NaCl and 2 ml of saturated Na_2CO_3 solution were added afterwards. The solution was extracted two times with 3

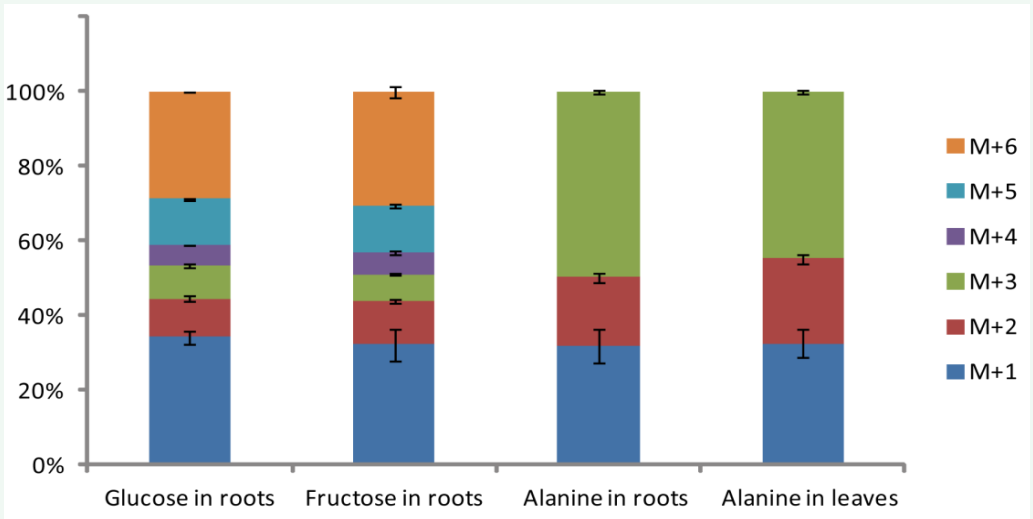

Figure 4 Isotopomer contribution for protein bound alanine and free sugars from the roots and leaves of $^{13}C_2$-labeled *P. ginseng*, respectively, as measured by GC/MS analysis. Isotopomers are shown as M+1 up to M+6 indicating molecules with one up to six ^{13}C-atoms, respectively. Error bars indicate standard deviations from three independent measurements.

ml ethyl acetate. The organic phase was dried under a constant stream of nitrogen. 200 µl of a 1:1 mixture of ethyl acetate and acetic anhydride was added to the dry residue and incubated over night at 60 °C in a sealed GC/MS vial. GC/MS analysis was done in split mode (1:5) with a temperature gradient from 150 ° (3 min) - 280 °C (10 °C/min). Other conditions were the same as described for amino acids. Under these conditions sucrose is hydrolysed, and analysed as glucose and fructose. The retention times for the glucose and fructose derivatives are 8.4 min and 7.9 min, respectively.

GC/MS analysis of ginsenosides

For hydrolysis of the ginsenosides, 50 mg of the freeze dried root sample were extracted with 1 ml of methanol. After drying, the residue was incubated at 90 °C for 3 h in 2.5 ml n-butanol containing 70 mg of sodium methoxide. After centrifugation, the butanolic phase was washed with 1.4 ml water. Afterwards, the organic layer was dried under a constant stream of nitrogen. The resulting aglycones were derivatized with a mixture of 30 µl BSTFA, 30 µl TMS and 20 µl TMS-Cl at 70 °C for 20 min. GC/MS analysis started with an oven temperature of 200 °C which was ramped at 30 °C/min to 300 °C which was then held for further 20 min other conditions were the same as described for amino acids. The retention times for the silylated panaxadiol and panaxatriol were 17.8 and 19.5 min, respectively. Characteristic m/z values, which were used for SIM analysis were 199 (C20-C27) and 593 (C1-C21) for panaxadiol, and 199 and 681 for panaxatriol.

RESULTS AND DISCUSSION

To study the biosynthetic origin of the ginsenosides Rg_1 and Rb_1 in full plants of *P. ginseng* under quasi-physiological conditions, we exposed a six-year-old plant in the field for 7 h (pulse period) to an atmosphere containing 700 ppm $^{13}CO_2$ (Figure 3A). During this period, the $^{13}CO_2$ concentration was monitored and held constant by continuously adding $^{13}CO_2$ from a gas bottle reservoir. After a chase period of 8 days, where the plant was further cultivated in the field under standard conditions (i.e. without a $^{13}CO_2$-enriched atmosphere), the roots were harvested (Figure 3B).

At the onset of the experiment, it was not clear whether the experimental approach using the relatively short 7 h $^{13}CO_2$-pulse to the six-year-old *P. ginseng* plant was sufficient to provide detectable and specific ^{13}C-enrichments in the root metabolites. As mentioned above, the approach crucially depends on the presence of multiple ^{13}C-labeled biosynthetic precursors in dilution with corresponding unlabeled building units at the site of biosynthesis. In the present project, this implied transport of sufficient amounts of ^{13}C-photosynthates (e.g. multiply ^{13}C-labeled sugars and related compounds formed during the relatively short pulse period of 7 h) from the leaves *via* the phloem into the roots where, during the chase period of 8 days, sufficient amounts of the target compounds (i.e. ginsenosides) must be biosynthesized in ^{13}C-labeled form. Notably, it can be assumed that the roots of the six-year-old plant already contained huge amounts of unlabeled ginsenosides that dilute the presumably tiny amounts of newly made metabolites during the experimental period of 8 days. On this basis, it was completely unknown whether a multiple ^{13}C-labeled ginsenoside could be detected at all with this setting.

To first provide information about ^{13}C-incorporation of $^{13}CO_2$ and the transfer of its photosynthates from the leaves into the roots, protein-derived amino acids from the roots were analyzed by GC/MS in the form of silylated derivatives. With the chosen setting (i.e. $^{13}CO_2$ pulse period of 7 h followed by a chase period of 8 days), ^{13}C-enrichments were fortunately detected for protein-bound amino acids. Particularly, 0.9 % ^{13}C-excess over the natural ^{13}C-abundance was detected for alanine from the roots, which was only slightly lower than ^{13}C-enrichment in alanine from the leaves (Figure 4). In both samples, about 50 % of labeled alanine was due to [U-$^{13}C_3$]-alanine. Completely ^{13}C-labeled alanine may

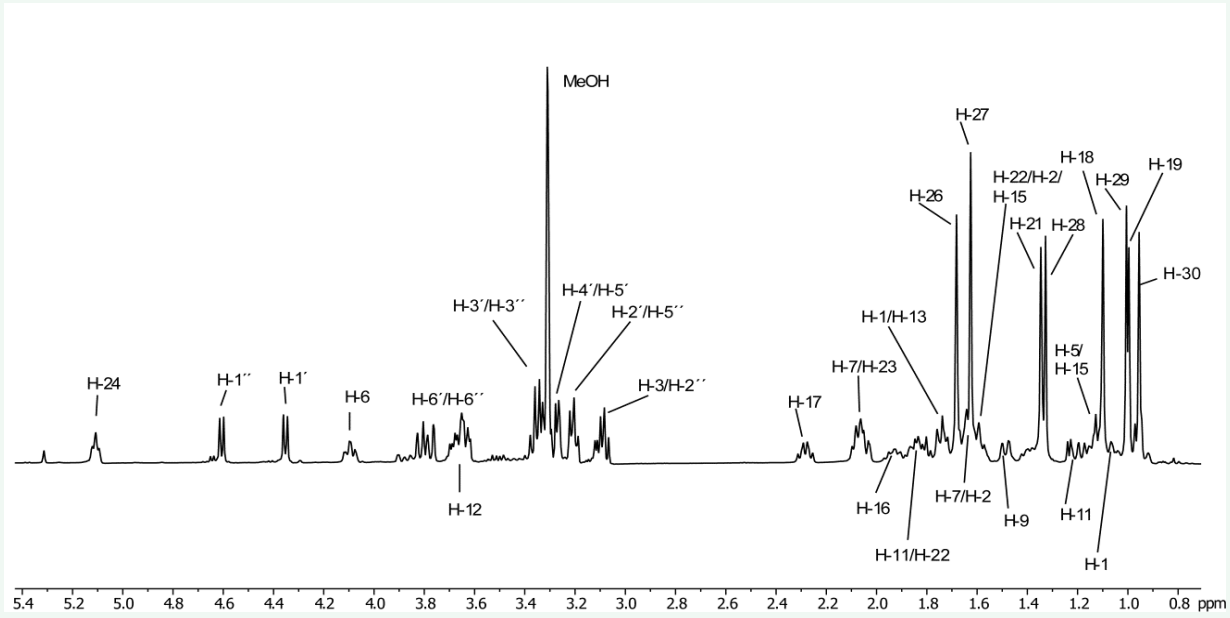

Figure 5 ^{1}H- NMR spectrum of Rg_1 from $^{13}CO_2$-labeled *P. ginseng* measured in deuterated methanol.

Table 1: ^{1}H and ^{13}C NMR signal assignments of the ginsenosides Rg_1 and Rb_1.

		Rg_1		Rb_1	
Aglycon	**C-Atom**	**^{1}H (δ) [ppm]**	**^{13}C (δ) [ppm]**	**^{1}H (δ) [ppm]**	**^{13}C (δ) [ppm]**
	1	1.06 1.74	40.31	1.03 1.74	40.31
	2	1.59	27.38	1.74 2.02	27.38
	3	3.11	79.98	3.21	79.98
	4		40.5		40.5
	5	1.12	61.9	0.79	61.9
	6	4.1	81	1.58	81.00
	7	1.64 2.04	45.4.0	1.31 1.56	45.40
	8		42.00		42.00
	9	1.48	50.73	1.44	50.73
	10		40.64		40.64
	11	1.19 1.85	31.08	1.25 1.80	31.08
	12	3.68	72.01	3.74	72.01
	13	1.74	49.78	1.75	49.78
	14		52.58		52.58
	15	1.13 1.60	31.67	1.05 1.59	31.67
	16	1.40 1.93	27.72	1.35 1.91	27.72
	17	2.29	53.26	2.30	53.26
	18	1.10	17.78	1.01	17.78
	19	0.99	17.97	0.87	17.97
	20		85.06		85.06
	21	1.35	22.97	1.38	22.97
	22	1.62 1.81	36.77	1.56 1.81	36.77
	23	2.07	24.39	2.05 2.15	24.39
	24	5.11	125.98	5.16	125.98
	25		132.43		132.43
	26	1.68	26.04	1.71	26.04
	27	1.63	18.11	1.65	18.11
	28 (α-Me)	1.33	31.51	1.09	31.51
	29 (β-Me)	1.02	16.25	0.87	16.25
	30	0.95	17.22	0.93	17.22
Sugars	**Glucose´**				
	1´	4.35	105.7	4.45	105.7
	2´	3.21	75.63	3.58	75.63
	3´	3.34	79.21	3.37	79.21
	4´	3.27	71.82	3.22	71.82
	5´	3.27	77.81		77.81
	6´	3.64 3.8	63.03	3.87	63.03
	Glucose´´				
	1´´	4.61	98.43	4.61	98.23
	2´´	3.08	75.53	3.13	
	3´´	3.36	78.34		
	4´´	3.31	71.32		
	5´´	3.21	78.07	3.44	
	6´´	3.65 3.82	62.65	3.81	70.35
	Glucose´´´				
	1´´´			4.69	104.57
	2´´´			3.24	76.44
	3´´´			3.58	78.64
	4´´´			3.36	71.61
	5´´´			3.28	78.02
	6´´´			3.65	63.26
	Glucose´´´´				
	1´´´´			4.37	105.14
	2´´´´			3.23	
	6´´´´			3.67	62.94

be used as a positive control to document the formation of [U-$^{13}C_3$]-phosphoglycerate from $^{13}CO_2$ during the photosynthetic process which can be further converted via [U-$^{13}C_3$]-GAP into [U-$^{13}C_3$]-pyruvate serving as the precursor for [U-$^{13}C_3$]-alanine and for [U-$^{13}C_2$] acetyl-CoA. Notably, [U-$^{13}C_2$] acetyl-CoA, [U-$^{13}C_3$]-pyruvate and [U-$^{13}C_3$]-GAP provide the carbon units for terpenes in the mevalonate and the MEP pathway, respectively (see below).

Additional evidence for the transfer of multiple ^{13}C-labeled photosynthates into root metabolites was provided by the labeling profiles of free glucose and fructose, which may partly derive from sucrose. As shown by GC/MS analysis, both sugars from the roots acquired significant ^{13}C-labels with ^{13}C-excess values of 2.3 %. About 30 % of labeled glucose and fructose were completely ^{13}C-labeled (Figure 4), reflecting their formation via $^{13}C_3$-carbon substrates.

Taken together, these data showed that the ^{13}C-label was readily transported from the leaves to the roots of the *Panax* plant presumably also providing specifically ^{13}C-labeled precursor units for ginsenoside biosynthesis. With this positive result in mind, we have now extracted and isolated ginsenosides from the roots of the $^{13}CO_2$-labeled plant. HPLC analysis showed that the protopanaxatriol-type Rg_1 and the protopanaxadiol-type Rb_1 were the most abundant ginsenosides in the methanolic extract of the six-year-old *P. ginseng* roots with 32.1 and 15.3 mg/g of fresh root material, respectively.

Fractionation of the crude methanolic root extract using preparative reversed phase HPLC yielded the ginsenosides Rb_1 and Rg_1 in good purity at amounts of about 10 mg and 5 mg, respectively, per g of root material. In total, about 100 mg of Rg_1 and 50 mg of Rb_1 were obtained in pure form. GC/MS analysis of the TMS derivatives of panaxadiol and panaxatriol from Rb_1 and Rg_1, respectively, as well as quantification of ^{13}C coupled satellites for H-24 in the ^1H NMR spectra showed less than 1 % ^{13}C excess. Due to this low ^{13}C-enrichment, a more concise analysis of the isotope distribution in the carbocycles of ginsenosides was only possible by NMR spectroscopy.

One-dimensional ^1H and ^{13}C NMR spectra of labeled Rg_1 are shown in (Figures 5 and 6), respectively, documenting the purity of the ginsenoside with sharp signals. Similarly, the spectra of Rb_1 were of high quality. All ^1H and ^{13}C NMR signals were assigned by two-dimensional COSY, TOCSY, HMQC and HMBC spectra (Table 1).

Additional confirmation was provided by INADEQUATE and 1,1-ADEQUATE experiments (see below). The signal assignments were in agreement with published values [71].

During NMR analysis, it became obvious that many of the ^{13}C NMR signals in Rg_1 and Rb_1 from the $^{13}CO_2$ experiment displayed satellites due to couplings between adjacent ^{13}C-atoms (for examples, see Figure 7).

These satellites were remarkably sharp and did not display any evidence for additional fine splittings due to long-range couplings. This was especially important to exclude biosynthetic contributions from [U-$^{13}C_3$]-GAP in the MEP route of terpene biosynthesis (see below). The relative intensities of these satellites were typically about 8-17 % in the overall signal intensity of a given ^{13}C NMR signal (Table 2), thus clearly exceeding the expected values due to statistical ^{13}C-^{13}C couplings (1 %) in natural ^{13}C-abundance compounds.

Obviously, these couplings were due to *de novo* synthesis of the ginsenosides via multiply ^{13}C-labeled precursors from $^{13}CO_2$ (see below). Remarkably, however, the intensities of the satellite pairs were higher in the ^{13}C NMR signals of Rg_1 (14.3 % ± 4.1 %) than in the corresponding ones in Rb_1 (8.9 % ± 2.6 %).This suggested that the protopanaxatriol-based Rg_1 was more efficiently biosynthesized during the pulse/chase experiment with the six-year-old plant. On this basis, it can be speculated whether higher amounts of the diol-based ginsenoside including Rb_1 were already present at the onset of the labeling experiment and whether higher oxidized ginsenosides including Rg_1 are preferably made in the older state of the *Panax* roots (i.e. in the six-year-old plant).

Some of satellites pairs in the ^{13}C NMR spectra of both ginsenosides were considerably lower (3-4 %) or even below the detection limit of the NMR sensitivity (< 3 %) (Table 2). Obviously, carbon atoms with this ^{13}C signature did not significantly acquire ^{13}C-label by adjacent $^{13}C_2$-units. On the basis of the specific coupling constants (Table 2) and on the basis of the specific correlations detected in two-dimensional INADEQUATE and ADEQUATE spectra (Figures 8 and 9), twelve $^{13}C_2$-isotopologues with adjacent ^{13}C-atoms were identified in the triterpene aglycons of Rg_1 and Rb_1, respectively (Figure 10, Table 2).

Some signals for the sugar moieties in Rg_1 and Rb_1 overlapped and the corresponding couplings could not be resolved. However, the signals for the C-1 and C-2 sugar carbon atoms were resolved showing ^{13}C-couplings to the neighbored carbon atoms. Closer inspection of the coupling pairs for C-1 revealed evidence for long range ^{13}C-coupling (i.e. coupling between C-1 and C-3 in the sugar moiety) due to the presence of [1,2,3-$^{13}C_3$]-sugars or isotopologues bearing more than three ^{13}C-atoms. This was also confirmed by the coupling patterns of the C-2' and C-2'' signals of the glucose moieties in Rg_1 where doublet of doublets due to simultaneous ^{13}C-coupling between ^{13}C-2 and its respective neighbors ^{13}C-1 and ^{13}C-3 (Figures 10 and 11). Thus, NMR analysis of the carbohydrate moieties in the ^{13}C-enriched ginsenosides again documented, as an internal control, the transfer of multiple ^{13}C-labeled precursors (i.e. with three and more ^{13}C-atoms in a given molecule) to the roots and the site of ginsenoside biosynthesis.

The observed ^{13}C-^{13}C coupling patterns were in perfect agreement with those predicted for a triterpene formed from [U-$^{13}C_2$] acetyl-CoA via the mevalonate pathway (Figure 12).

More specifically, twelve isotopologues with adjacent ^{13}C atoms, i.e. [2,3-$^{13}C_2$]-, [4,29-$^{13}C_2$]-, [5,6-$^{13}C_2$]-, [8,18-$^{13}C_2$]-, [9,11-$^{13}C_2$]-, [10,19-$^{13}C_2$]-, [12,13-$^{13}C_2$]-, [14,30-$^{13}C_2$]-, [16,17-$^{13}C_2$]-, [20,21-$^{13}C_2$]-, [23,24-$^{13}C_2$]-, and [25,27-$^{13}C_2$]- isotopologues can be predicted on the basis of the mevalonate route and the established mechanisms of ring formation starting from the chair-chair-chair-boat conformation of the (S)-2,3-oxidosqualene precursor and with the dammarenyl cation as an intermediate of

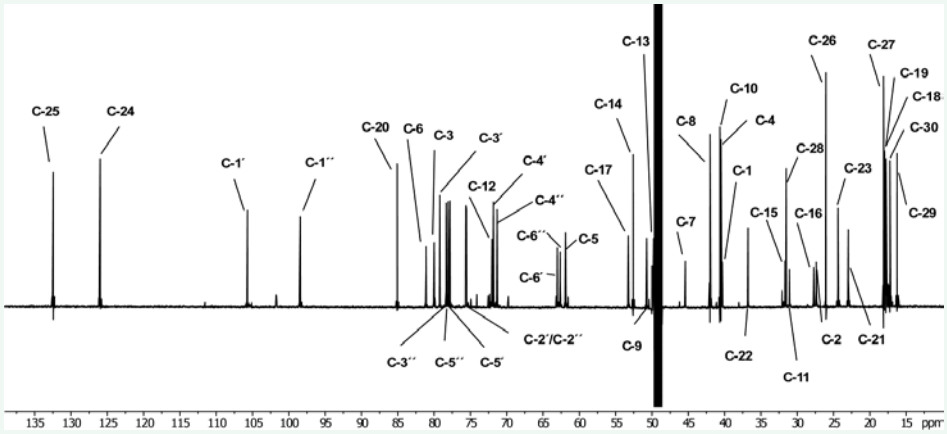

Figure 6 Overall ^{13}C-NMR spectrum of Rg_1 from $^{13}CO_2$-labeled *P. ginseng* measured in deuterated methanol.

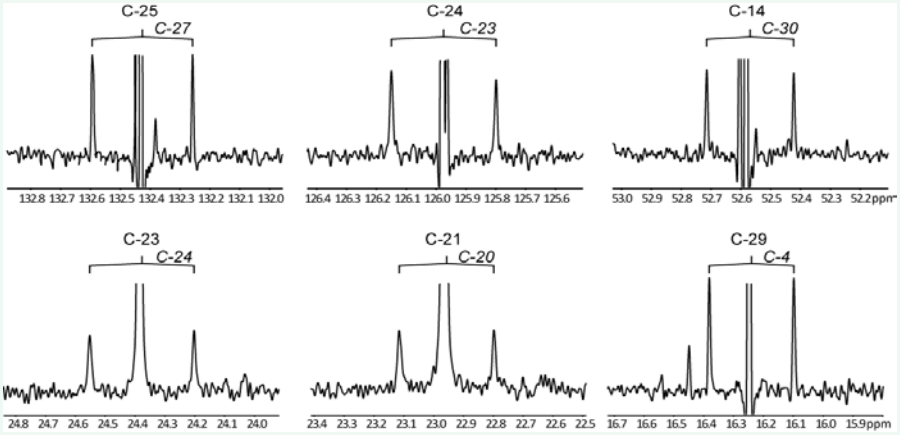

Figure 7 Expanded view of some ^{13}C- NMR signals of Rg_1 from the $^{13}CO_2$ experiment. Satellite pairs due to ^{13}C-^{13}C couplings are indicated. Simultaneous couplings between three ^{13}C-atoms were not observed as shown by the "empty" down-field and up-field regions of the coupling pairs. Long-range ^{13}C-couplings indicative of the MEP-pathway were also not detected. The spectrum was calculated after zero-filling and multiplication of the FID with a Gaussian function to achieve sharp signals.

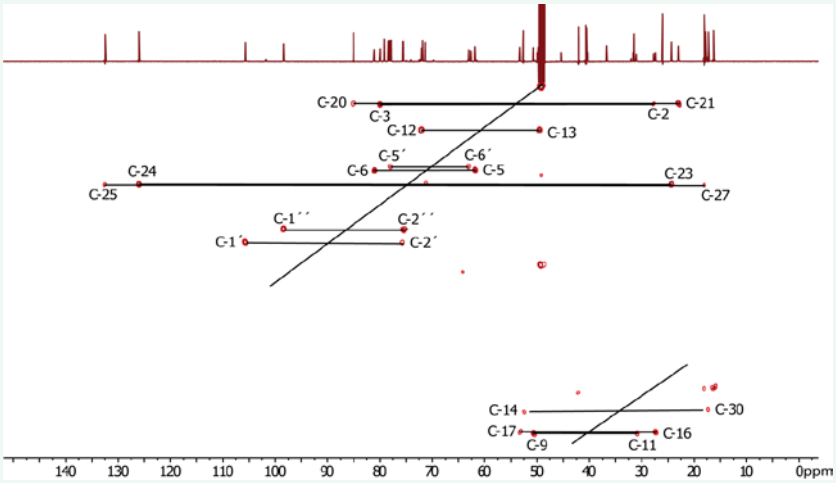

Figure 8 INADEQUATE spectrum of Rg_1 from the $^{13}CO_2$ experiment. Observed correlations (connected by horizontal lines in the two-dimensional matrix) reflect the biosynthetic history of the ginsenoside from $^{13}CO_2$ and are due to magnetization transfer of a ^{13}C-atom to a direct ^{13}C-neighbour (see also bold dark-blue bars in Figure 11). The one-dimensional ^{13}C-spectrum is shown as projections. Skip diagonals are also drawn as lines for the main part (upper part of the spectrum) and the folded region (lower part).

Table 2: NMR data of Rg_1 and Rb_1 from the $^{13}CO_2$ experiment. n.d., not determined due to signal overlap.

C-atom	Relative signal intensity of $^{13}C^{13}C$ satellites [%]		J_{CC} [Hz]		Correlation with	Confirmed (+) with	
	Rg_1	Rb_1	Rg_1	Rb_1		ADEQUATE Rg_1/Rb_1	INADEQUATE Rg_1/Rb_1
1	< 3	< 3	< 3	< 3			
2	12.6	3.0	32.6	36.5	3	+/+	+/+
3	12.3	6.6	36.5	37.4	2	+/+	+/+
4	13.3	10.4	36.0	35.5	29	+/+	
5	12.5	9.5	38.7	36.1	6	+/+	+/
6	14.2	12.0	38.8	38.7	5	+/+	+/
7	< 3	< 3	< 3	< 3			
8	10.3	7.0	36.6	36.8	18	+/+	
9	12.0	5.9	34.5	36.8	11	+/+	+/+
10	12.8	8.9	35.5	35.5	19	+/+	
11	17.1	8.9	34.9	36.5	9	+/+	+/+
12	13.5	n.d.	37.2	n.d.	13	+/+	+/+
13	7.5	n.d.	37.8	n.d.	12	+/	+/+
14	10.5	8.3	36.6	36.5	30	+/+	+/
15	< 3	< 3					
16	16.6	7.6	36.4	39.0	17	+/+	+/
17	9.5	4.4	32.5	33.5	16	+/+	+/
18	16.8	10.4	38.7	36.7	8	+/+	
19	28.5	9.8	43.7	40.3	10	+/+	
20	13.1	10.1	39.9	39.6	21	+/+	+/+
21	13.4	9.3	39.9	38.9	20	+/+	+/+
22	3.1	< 3	38.6				
23	13.4	7.3	44.3	44.1	24	+/+	+/
24	18.0	10.2	44.2	44.0	23	+/+	+/
25	17.8	14.1	42.4	42.3	27	+/+	+/
26	< 3	< 3					
27	13.6	12.2	42.4	42.5	25	+/+	+/
28 (α-Me)	4.0	< 3	35.0		4		
29 (β-Me)	16.5	11.7	36.2	39.2	4	+/+	
30	16.8	7.8	36.6	36.7	14	+/+	+/
Glucose							
1′	17.5	12.3	48.2	47.0	2′	+/+	+/
2′	8.0		47.7		1′	+/	+/
3′	3.1		42.1				
4′	18.2		41.4				
5′	8.1		42.1		6′	+/	+/
6′	27.9		43.1		5′	+/	+/
1′′	15.6	7.4	47.6	48.3	2′′	+/+	+/
2′′	6.1		46.9		1′′	+/	+/
3′′							
4′′	10.5		41.0				
5′′					6′′	+/	
6′′	15.7		42.6		5′′	+/	
1′′′		13.0		47.2	2′′′	/+	
1′′′′		14.0		44.3	2′′′′	/+	

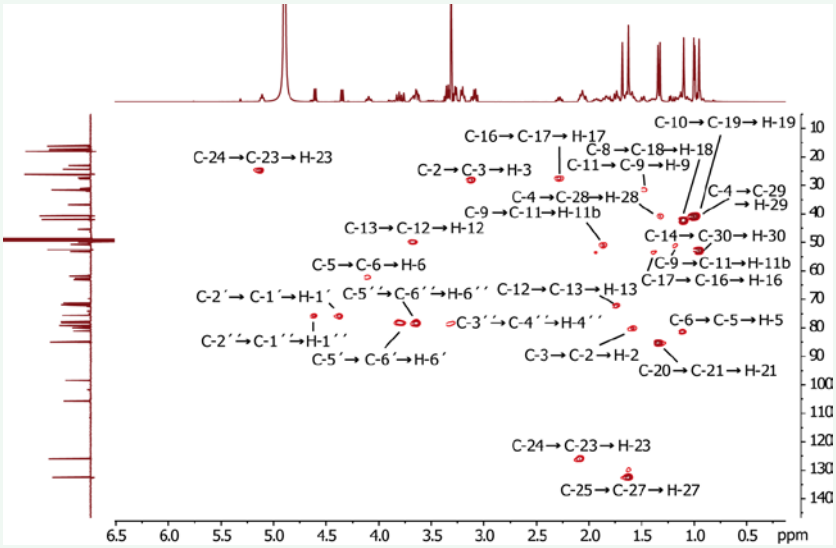

Figure 9 1, 1-ADEQUATE spectrum of Rg_1 from the $^{13}CO_2$ experiment. Observed correlations reflect the biosynthetic history of the ginsenoside from $^{13}CO_2$ and are due to magnetization transfer of a ^{13}C-atom to a direct ^{13}C-neighbour and its connected H-atom (see also green arrows in Figure 11). One-dimensional ^{1}H- and ^{13}C-spectra are shown as projections.

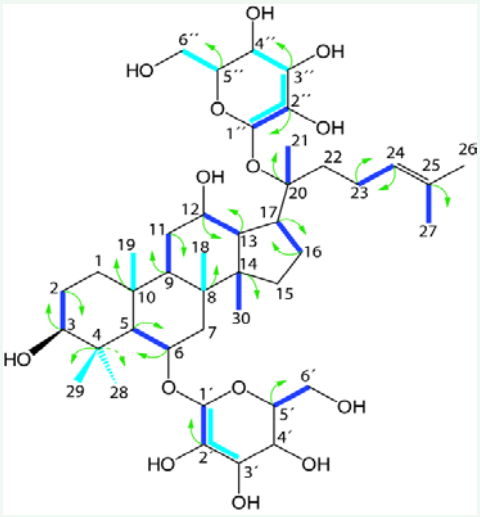

Figure 10 Labeling pattern of the ginsenoside Rg_1 from the $^{13}CO_2$ experiment; biosynthetically contributed ^{13}C atom pairs are indicated by bold lines. Dark-blue lines display ^{13}C-pairs observed in the INADEQUATE spectrum; green arrows indicate connections detected in the ADEQUATE spectrum. The weak signal observed between ^{13}C-4 and H-28 is indicated by the dotted green arrow. Additional ^{13}C-pairs or triples gleaned from the analysis of the coupling pattern in the one-dimensional ^{13}C-NMR spectrum are displayed by bright-blue lines.

the ginsenosides under study (Figure 13).

On the other hand, the MEP route involving a [U-$^{13}C_3$]-GAP precursor would have generated, in addition to the above mentioned isotopologues, six $^{13}C_3$-units, namely [2,3,28-$^{13}C_3$]-, [1,5,6-$^{13}C_3$]-, [7,9,11-$^{13}C_3$], [12,13,15-$^{13}C_3$], [16,17,22-$^{13}C_3$]- and [23,24,26-$^{13}C_3$]-isotopologues (indicated in red in Figure 12). Whereas the twelve $^{13}C_2$-pairs predicted by the mevalonate route were detected in the NMR data of Rg_1 and Rb_1, none of the $^{13}C_3$-isotopologues could be observed neither as long-range couplings in the one-dimensional ^{13}C NMR signals, even under extreme Gaussian processing of the FID, nor by two-dimensional n,1-ADEQUATE experiments (data not shown) optimized to detect adjacent $^{13}C_2$-units and an outlier ^{13}C, as predicted for the ginsenosides via the MEP route. Importantly, the labeling patterns of alanine, free sugars and the sugar moieties of the ginsensoides provided experimental proof for the formation of [U-$^{13}C_3$]-GAP during the pulse period and its transport to the roots where ginsenosides are made, but not its use for Rg_1 and Rb_1 biosynthesis. Therefore, it appears safe to assume that IPP and DMAPP used as precursors for the triterpene aglycons of Rg_1 and Rb_1 are predominantly, if not exclusively, made from the mevalonate pathway in the full-grown six-year-old plants of *P. ginseng*. Capitalizing on the detection limits of the experiment, it can be estimated that contributions of IPP and DMAPP via the

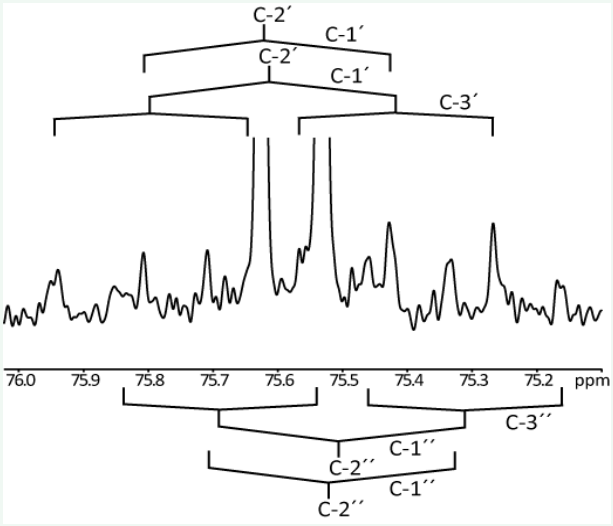

Figure 11 Expanded view of some ^{13}C-NMR sugar signals of Rg_1 from the $^{13}CO_2$ experiment. Satellite pairs due to ^{13}C-^{13}C couplings are indicated. Note the simultaneous couplings between three ^{13}C-atoms (see also bright-blue bars in Figure 10).

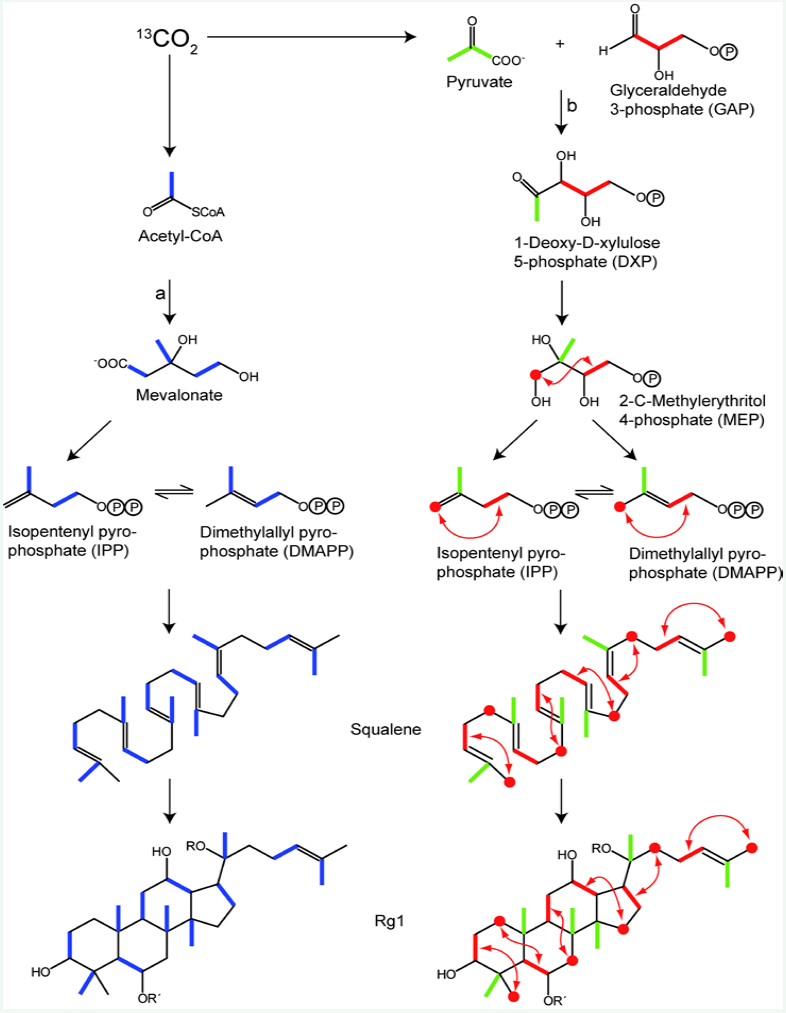

Figure 12 Predicted labeling patterns of the ginsenoside Rg_1 from $^{13}CO_2$-labeled plants of *P. ginseng*. The bold bonds indicate adjacent ^{13}C-atoms via the mevalonate pathway (**a**, from $^{13}C_2$-acetyl-CoA and mevalonate, colored in blue) or the MEP pathway (**b**, from $^{13}C_3$-pyruvate, colored in green, and $^{13}C_3$-GAP, colored in red; note that one of the ^{13}C-atoms in $^{13}C_3$-GAP becomes separated during the formation of MEP as indicated by filled red circles).

MEP pathway have to be far below 5 %, if at all. On this basis, the earlier observations [65] about significant contributions of the MEP pathway to ginsenoside biosynthesis might have reflected the studied [65] situation and adaptation processes of *Panax* hairy root cell cultures growing in an artificial medium containing specific inhibitors of the mevalonate and MEP pathway, respectively. Obviously, these factors are not relevant for the undisturbed and physiological *in planta* condition examined in our study.

CONCLUSION

Using $^{13}CO_2$ pulse/chase experiments in the field, we have shown that full grown six-year-old *P. ginseng* plants use the mevalonate pathway as the predominant, if not the exclusive route to synthesize the major ginsenosides Rg_1 and Rb_1. The labeling patterns confirm their formation via (S)-2,3-oxidosqualene and the dammarenyl cation as intermediates. The enzymes involved in these reactions are promising targets in improving the yields of ginsenosides by recombinant techniques. The labeling data also suggest that protopanaxatriol-based ginsenosides are biosynthesized late in the root development of the plant in comparison to panaxadiol-based ginsenosides.

The understanding of the location, timing and the pathways affording ginsenosides is important to optimize and modify plant lines for cultivation as well as for developing efficient biotechnological means to produce ginsenosidesn with cell cultures or recombinant organisms. Notably, the highest yields in the production of ginsenosides can still be found *in planta* in the roots of 6 year-old *P. ginseng*. This long-term cultivation period is a considerable cost factor in the commercial production of Ginseng drugs. Therefore, companies involved in the Ginseng business [in Germany, e.g. Florafarm GmbH both cultivating *P. ginseng* in plantations and producing Ginseng drugs/products which are directly distributed to the consumers (*www.florafarm.de*)] are interested in a shortened cultivation period while maintaining or even improving the yield and quality of their products. Knowledge about the natural biosynthetic process is therefore a crucial prerequisite to develop rational approaches in this optimization process.

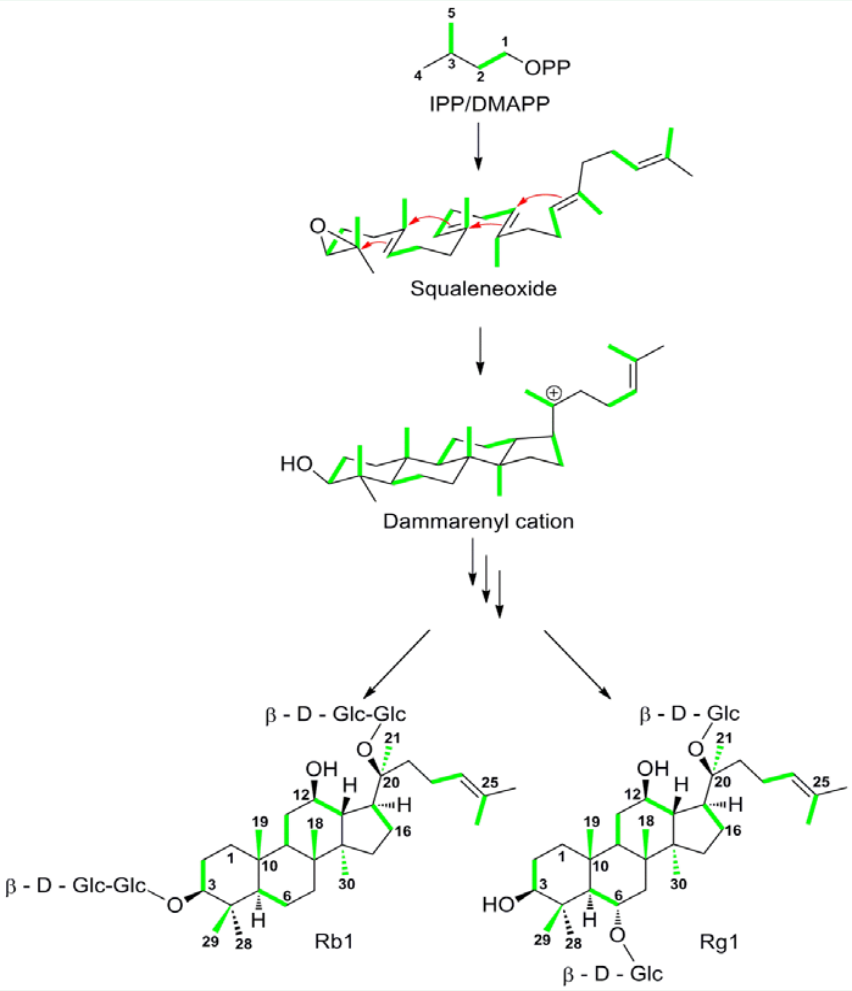

Figure 13 Biosynthesis of the ginsenosides Rg_1 and Rb_1 in full-grown plants of *P. ginseng*. Bold green lines indicate the adjacent ^{13}C-atom pairs that were contributed from $^{13}CO_2$ via [1,2-$^{13}C_2$]acetyl-CoA and [1,2-$^{13}C_2$]-, [3,5-$^{13}C_2$]-IPP/DMAPP. The labeling patterns of Rb_1 and Rg_1 were detected by NMR spectroscopy. Notably, the detected $^{13}C_2$-pair in C-4 and C-29 (β-methyl group at C-4) is indicative for the stereospecificity displayed in the figure.

ACKNOWLEDGEMENTS

We thank the Deutsche Forschungsgemeinschaft (EI 384/8-1) for financial support. L. M. P.-R. and W. E. thank the German Academic Exchange Service (DAAD, A/11/00471) and CONACYT-México (exp. No. 160813) for supporting the sabbatical stay of L. M. P.-R. at TUM. Financial support from the FOMIX-Yucatán Project No. 66262 and the Hans-Fischer Gesellschaft (München) is also gratefully acknowledged. We cordially thank Henrike Rodemeier and Dennis Koopmann from Florafarm GmbH for essential support when performing the field experiments at the Ginseng farm.

REFERENCES

1. Tilburt JC, Kaptchuk TJ. Herbal medicine research and global health: an ethical analysis. Bull World Health Organ. 2008; 86: 594-599.
2. WHO global strategy on traditional and alternative medicine. Public Health Rep. 2002; 117: 300-301.
3. Willcox ML, Bodeker G. Traditional herbal medicines for malaria. BMJ. 2004; 329: 1156-1159.
4. WHO traditional medicine strategy: 2014–2023. Geneva: World Health Organization; 2013.
5. Choi J, Kim TH, Choi TY, Lee MS. Ginseng for health care: a systematic review of randomized controlled trials in Korean literature. PLoS One. 2013; 8: e59978.
6. Kiefer D, Pantuso T. Panax ginseng. Am Fam Physician. 2003; 68: 1539-1542.
7. Baeg IH, So SH. The world ginseng market and the ginseng (Korea). J Ginseng Res. 2013; 37: 1-7.
8. Lee MH, Jeong JH, Seo JW, Shin CG, Kim YS, In JG, et al. Enhanced triterpene and phytosterol biosynthesis in Panax ginseng overexpressing squalene synthase gene. Plant Cell Physiol. 2004; 45: 976-984.
9. Liang Y, Zhao S. Progress in understanding of ginsenoside biosynthesis. Plant Biol (Stuttg). 2008; 10: 415-421.
10. Choi YE. Ginseng (Panax ginseng). Methods Mol Biol. 2006; 344: 361-371.
11. Leung KW, Wong AS. Pharmacology of ginsenosides: a literature review. Chin Med. 2010; 5: 20.
12. Podolak I, Galanty A, Sobolewska D. Saponins as cytotoxic agents: a review. Phytochem Rev. 2010; 9: 425-474.
13. Christensen LP. Ginsenosides chemistry, biosynthesis, analysis, and potential health effects. Adv Food Nutr Res. 2009; 55: 1-99.
14. Kim HG, Yoo SR, Park HJ, Lee NH, Shin JW, Sathyanath R, et al. Antioxidant effects of Panax ginseng C.A. Meyer in healthy subjects: a randomized, placebo-controlled clinical trial. Food Chem Toxicol. 2011; 49: 2229-2235.
15. Shin HR, Kim JY, Yun TK, Morgan G, Vainio H. The cancer-preventive potential of Panax ginseng: a review of human and experimental evidence. Cancer Causes Control. 2000; 11: 565-576.
16. Lee JH, Choi SH, Kwon OS, Shin TJ, Lee JH, Lee BH, et al. Effects of ginsenosides, active ingredients of Panax ginseng, on development, growth, and life span of Caenorhabditis elegans. Biol Pharm Bull. 2007; 30: 2126-2134.
17. Paul S, Shin HS, Kang SC. Inhibition of inflammations and macrophage activation by ginsenoside-Re isolated from Korean ginseng (Panax ginseng C.A. Meyer). Food Chem Toxicol. 2012; 50: 1354-1361.
18. Hong SY, Kim JY, Ahn HY, Shin JH, Kwon O. Panax ginseng extract rich in ginsenoside protopanaxatriol attenuates blood pressure elevation in spontaneously hypertensive rats by affecting the Akt-dependent phosphorylation of endothelial nitric oxide synthase. J Agric Food Chem. 2012; 60: 3086-3091.
19. Raghavendran HR, Sathyanath R, Shin J, Kim HK, Han JM, Cho J, et al. Panax ginseng modulates cytokines in bone marrow toxicity and myelopoiesis: ginsenoside Rg1 partially supports myelopoiesis. PLoS One. 2012; 7: e33733.
20. Jung ID, Kim HY, Park JW, Lee CM, Noh KT, Kang HK, et al. RG-II from Panax ginseng C.A. Meyer suppresses asthmatic reaction. BMB Rep. 2012; 45: 79-84.
21. Gum SI, Jo SJ, Ahn SH, Kim SG, Kim JT, Shin HM, et al. The potent protective effect of wild ginseng (Panax ginseng C.A. Meyer) against benzo[alpha]pyrene-induced toxicity through metabolic regulation of CYP1A1 and GSTs. J Ethnopharmacol. 2007; 112: 568-576.
22. Helms S. Cancer prevention and therapeutics: Panax ginseng. Altern Med Rev. 2004; 9: 259-274.
23. Yue PY, Mak NK, Cheng YK, Leung KW, Ng TB, Fan DT, et al. Pharmacogenomics and the Yin/Yang actions of ginseng: anti-tumor, angiomodulating and steroid-like activities of ginsenosides. Chin Med. 2007; 2: 6.
24. Augustin JM, Kuzina V, Andersen SB, Bak S. Molecular activities, biosynthesis and evolution of triterpenoid saponins. Phytochemistry. 2011; 72: 435-457.
25. Jia L, Zhao Y, Liang XJ. Current evaluation of the millennium phytomedicine- ginseng (II): Collected chemical entities, modern pharmacology, and clinical applications emanated from traditional Chinese medicine. Curr Med Chem. 2009; 16: 2924-2942.
26. Liu J, Wang Y, Qiu L, Yu Y, Wang C. Saponins of Panax notoginseng: chemistry, cellular targets and therapeutic opportunities in cardiovascular diseases. Expert Opin Investig Drugs. 2014; 23: 523-539.
27. Dinda B, Debnath S, Mohanta BC, Harigaya Y. Naturally occurring triterpenoid saponins. Chem Biodivers. 2010; 7: 2327-2580.
28. Shibata S. Chemistry and cancer preventing activities of ginseng saponins and some related triterpenoid compounds. J Korean Med Sci. 2001; 16 Suppl: S28-37.
29. Kim SJ, Yuan HD, Chung SH. Ginsenoside Rg1 suppresses hepatic glucose production via AMP-activated protein kinase in HepG2 cells. Biol Pharm Bull. 2010; 33: 325-328.
30. Liang J, Yu Y, Wang B, Lu B, Zhang J, Zhang H, Ge P. Ginsenoside Rb1 attenuates oxygen-glucose deprivation-induced apoptosis in SH-SY5Y cells via protection of mitochondria and inhibition of AIF and cytochrome c release. Molecules. 2013; 18: 12777-12792.
31. Huang SL, He XJ, Li ZF, Lin L, Cheng B. Neuroprotective effects of ginsenoside Rg1 on oxygen-glucose deprivation reperfusion in PC12 cells. Pharmazie. 2014; 69: 208-211.
32. Ni N, Liu Q2, Ren H3, Wu D4, Luo C5, Li P6, Wan JB7. Ginsenoside

Rb1 protects rat neural progenitor cells against oxidative injury. Molecules. 2014; 19: 3012-3024.

33. Zhang Y, Sun K, Liu YY, Zhang YP, Hu BH, Chang X, et al. Ginsenoside Rb1 ameliorates lipopolysaccharide-induced albumin leakage from rat mesenteric venules by intervening in both trans- and paracellular pathway. Am J Physiol - Gast Liver Physiol. 2014; 306: G289-G300.

34. Haralampidis K, Trojanowska M, Osbourn AE. Biosynthesis of triterpenoid saponins in plants. Adv Biochem Eng Biotechnol. 2002; 75: 31-49.

35. Thimmappa R, Geisler K, Louveau T, O'Maille P, Osbourn A. Triterpene biosynthesis in plants. Annu Rev Plant Biol. 2014; 65: 225-257.

36. Jenner H, Townsend B, Osbourn A. Unravelling triterpene glycoside synthesis in plants: phytochemistry and functional genomics join forces. Planta. 2005; 220: 503-506.

37. Osbourn A, Goss RJ, Field RA. The saponins: polar isoprenoids with important and diverse biological activities. Nat Prod Rep. 2011; 28: 1261-1268.

38. Sawai S, Saito K. Triterpenoid biosynthesis and engineering in plants. Front Plant Sci. 2011; 2: 25.

39. Han JY, In JG, Kwon YS, Choi YE. Regulation of ginsenoside and phytosterol biosynthesis by RNA interferences of squalene epoxidase gene in Panax ginseng. Phytochemistry. 2010; 71: 36-46.

40. Han JY, Kwon YS, Yang DC, Jung YR, Choi YE. Expression and RNA interference-induced silencing of the dammarenediol synthase gene in Panax ginseng. Plant Cell Physiol. 2006; 47: 1653-1662.

41. Hu W, Liu N, Tian Y, Zhang L. Molecular cloning, expression, purification, and functional characterization of dammarenediol synthase from Panax ginseng. Biomed Res Int. 2013; 2013: 285740.

42. Tansakul P, Shibuya M, Kushiro T, Ebizuka Y. Dammarenediol-II synthase, the first dedicated enzyme for ginsenoside biosynthesis, in Panax ginseng. FEBS Lett. 2006; 580: 5143-5149.

43. Kushiro T, Ohno Y, Shibuya M, Ebizuka Y. In vitro conversion of 2,3-oxidosqualene into dammarenediol by Panax ginseng microsomes. Biol Pharm Bull. 1997; 20: 292-294.

44. Kushiro T, Shibuya M, Ebizuka Y. Beta-amyrin synthase--cloning of oxidosqualene cyclase that catalyzes the formation of the most popular triterpene among higher plants. Eur J Biochem. 1998; 256: 238-244.

45. Xue Z, Duan L, Liu D, Guo J, Ge S, Dicks J, et al. Divergent evolution of oxidosqualene cyclases in plants. New Phytol. 2012; 193: 1022-1038.

46. Han JY, Kim HJ, Kwon YS, Choi YE. The Cyt P450 enzyme CYP716A47 catalyzes the formation of protopanaxadiol from dammarenediol-II during ginsenoside biosynthesis in Panax ginseng. Plant Cell Physiol. 2011; 52: 2062-2073.

47. Han JY, Hwang HS, Choi SW, Kim HJ, Choi YE. Cytochrome P450 CYP716A53v2 catalyzes the formation of protopanaxatriol from protopanaxadiol during ginsenoside biosynthesis in Panax ginseng. Plant Cell Physiol. 2012; 53: 1535-1545.

48. Han JY, Kim MJ, Ban YW, Hwang HS, Choi YE. The involvement of Î²-amyrin 28-oxidase (CYP716A52v2) in oleanane-type ginsenoside biosynthesis in Panax ginseng. Plant Cell Physiol. 2013; 54: 2034-2046.

49. Bochar DA, Friesen JA, Stauffacher CV, Rodwell VW. Biosynthesis of mevalonic acid from acetyl-CoA. Cane DE, editor. In: Comprehensive natural product chemistry. Oxford: Pergamon. 1999; 15-44.

50. Bloch K. Sterol molecule: structure, biosynthesis, and function. Steroids. 1992; 57: 378-383.

51. Bach TJ. Some new aspects of isoprenoid biosynthesis in plants--a review. Lipids. 1995; 30: 191-202.

52. Qureshi N, Porter JW. Conversion of acetyl-coenzyme A to isopentenyl pyrophosphate. Porter JW, Spurgeon SL, editors. In: Biosynthesis of isoprenoid compounds. New York: John Wiley. 1981; 47-94.

53. Kuzuyama T, Seto H. Two distinct pathways for essential metabolic precursors for isoprenoid biosynthesis. Proc Jpn Acad Ser B Phys Biol Sci. 2012; 88: 41-52.

54. Gräwert T, Groll M, Rohdich F, Bacher A, Eisenreich W. Biochemistry of the non-mevalonate isoprenoid pathway. Cell Mol Life Sci. 2011; 68: 3797-3814.

55. Rohmer M. A mevalonate-independent rout to isopentenyl diphosphate. Cane DE, editor. In: Comprehensive natural product chemistry. Oxford: Pergamon. 1999; 45-68.

56. Eisenreich W, Bacher A, Arigoni D, Rohdich F. Biosynthesis of isoprenoids via the non-mevalonate pathway. Cell Mol Life Sci. 2004; 61: 1401-1426.

57. Schramek N, Wang H, Römisch-Margl W, Keil B, Radykewicz T, Winzenhörlein B, et al. Artemisinin biosynthesis in growing plants of Artemisia annua. A 13CO2 study. Phytochemistry. 2010; 71: 179-187.

58. Hemmerlin A, Hoeffler JF, Meyer O, Tritsch D, Kagan IA, Grosdemange-Billiard C, et al. Cross-talk between the cytosolic mevalonate and the plastidial methylerythritol phosphate pathways in tobacco bright yellow-2 cells. J Biol Chem. 2003; 278: 26666-26676.

59. Arigoni D, Sagner S, Latzel C, Eisenreich W, Bacher A, Zenk MH. Terpenoid biosynthesis from 1-deoxy-D-xylulose in higher plants by intramolecular skeletal rearrangement. Proc Natl Acad Sci U S A. 1997; 94: 10600-10605.

60. Hemmerlin A, Harwood JL, Bach TJ. A raison d'être for two distinct pathways in the early steps of plant isoprenoid biosynthesis? Prog Lipid Res. 2012; 51: 95-148.

61. Aharoni A, Jongsma MA, Bouwmeester HJ. Volatile science? Metabolic engineering of terpenoids in plants. Trends Plant Sci. 2005; 10: 594-602.

62. Flügge UI, Gao W. Transport of isoprenoid intermediates across chloroplast envelope membranes. Plant Biol (Stuttg). 2005; 7: 91-97.

63. Peña-Rodríguez LM, Yam-Puc A, Knispel N, Schramek N, Huber C, Graßberger C, et al. Isotopologue profiling of triterpene formation under physiological conditions. Biosynthesis of lupeol-3-(3'-R-hydroxy)-stearate in Pentalinon andrieuxii. J Org Chem. 2014; 79: 2864-2873.

64. Chaurasiya ND, Sangwan NS, Sabir F, Misra L, Sangwan RS. Withanolide biosynthesis recruits both mevalonate and DOXP pathways of isoprenogenesis in Ashwagandha Withania somnifera L. (Dunal). Plant Cell Rep. 2012; 31: 1889-1897.

65. Zhao S, Wang L, Liu L, Liang Y, Sun Y, Wu J. Both the mevalonate and the non-mevalonate pathways are involved in ginsenoside biosynthesis. Plant Cell Rep. 2014; 33: 393-400.

66. Eisenreich W, Huber C, Kutzner E, Knispel N, Schramek N. Isotopologue

Profiling–Towards a better understanding of metabolic pathways. Weckwerth W, Kahl G, editors. In: Handbook of Plant Metabolomics, New York: Wiley-Blackwell. 2013; 25–56.

67. Römisch-Margl W, Schramek N, Radykewicz T, Ettenhuber C, Eylert E, Huber C, et al. 13CO2 as a universal metabolic tracer in isotopologue perturbation experiments. Phytochemistry. 2007; 68: 2273-2289.

68. Knispel N, Ostrozhenkova E, Schramek N, Huber C, Peña-Rodríguez LM, Bonfill M, et al. Biosynthesis of panaxynol and panaxydol in Panax ginseng. Molecules. 2013; 18: 7686-7698.

69. Ostrozhenkova E, Eylert E, Schramek N, Golan-Goldhirsh A, Bacher A, Eisenreich W. Biosynthesis of the chromogen hermidin from Mercurialis annua L. Phytochemistry. 2007; 68: 2816-2824.

70. Ginseng. In European Pharmacopeia 8.0, edqm, 2014; 1261.

71. Lin MC, Wang KC, Lee SS. Transformation of ginsenosides Rg1 and Rb, and crude Sanchi saponins by human intestinal microflora. J. Chin. Chem. Soc. 2001; 48: 113-120.

Cite this article

Schramek N, Huber C, Schmidt S, Dvorski SEM, Knispel N, et al. (2014) Biosynthesis of Ginsenosides in Field-Grown Panax Ginseng. JSM Biotechnol Bioeng 2(1): 1033.